Laser-Action in V-Groove–Shaped InGaAs–InP Single Quantum Wires

Dirk Piester, Peter Bönsch, Thomas Schrimpf, Hergo-Heinrich Wehmann, and Andreas Schlachetzki

***Abstract*—We report on the realization of a V-groove–shaped single quantum wire (QWR) laser in the material system InGaAsP–InP. First, we discuss a new laser concept that makes use of a semi-insulating (s.i.) current-blocking layer and InGaAsP wave-guiding layers. Simulations demonstrate the concentration of both the current as well as the optical field in the active region. We developed a two-step wet-chemical etching process, to form high-quality V-grooves into a layer stack consisting of InP and InGaAsP. By employing anisotropic wet-chemical etching and anisotropic metal-organic vapor-phase epitaxial (MOVPE) growth, we demonstrate the feasibility of this concept. We show laser action originating from a single InGaAs QWR realized in this concept. The source of a second laser line measured with electroluminescence (EL) spectroscopy is discussed.**

***Index Terms*—InP, MOVPE, quantum wire laser, V-groove, wet-chemical etching.**

I. Introduction

DURING the last decade, low-dimensional semiconductor structures find wide applications in optoelectronic devices. A prominent example is their use as active regions in lasers. Quantum structure lasers are expected to show improved device properties, such as low threshold current, high optical gain [1], and low temperature sensitivity [2]. Thus, they are of special interest for monolithic integration with multilaser applications and low-power electronics.

The advantageous features of quantum wires (QWR's) are enhanced compared with quantum wells (QWL's) with their quantum confinement in only one dimension. On the other hand, quantum dots (QD's) being confined in three dimensions should be superior to QWR's, but such structures are commonly realized by self-organized epitaxial growth [3]–[5]. Thus, they are statistically distributed in size and area. Eluding this statistical growth, QWR's can be formed in a well-controlled manner just as QWL's by pursuing suitable concepts. Further, the capability of growing lattice-matched QWR's offers an additional degree of freedom in structural design and material selection.

Until now, many efforts have been devoted to the realization of QWR lasers. An example is the use of self-organized growth [6], [7]. In the case of GaAs–AlGaAs QWR's, the growth was carried out by molecular beam epitaxy (MBE) on (775)B-oriented substrates. A comparison with a similar QWL structure shows that the threshold current of the QWR laser is by far smaller than that of the QWL laser [6]. Additional possibilities are the growth on a ridge structure [8], the growth on multiatomic steps [9], or the structuring of QWR's by means of electron beam lithography [10]. All of these works require particularly demanding technological processes or are based on lattice mismatch.

A further important method is the anisotropic growth on V-groove patterned substrates [11]. Promising is the design published by Toda *et al.* [12], comprising a QWR DFB laser in the InAsP–InP system. In this case, mass transport of group III elements during growth is purposefully used. Until now, the lowest threshold current measured with a QWR laser is 188 μA at room temperature [13]. This was achieved in the V-groove concept with an InGaAs QWR on GaAs substrate.

Most QWR lasers on patterned substrates were grown on GaAs with GaAs–AlGaAs [14], [15] and InGaAs–AlGaAs [13] layers with emission wavelengths of about 840 and 980 nm, respectively. This wavelength range extending even up to 1.3 μm can also be covered by InGaAs–GaAs QD's [5]. However, only In(Ga)As(P)–InP has been experimentally demonstrated for lasers in the 1.55-μm wavelength region [7], [12]. But in comparison with AlGaAs, which is nearly lattice-matched for all compositions to a GaAs substrate, the composition of InGaAs(P) must be controlled precisely to avoid crystal defects. Another problem is the mass transport during the heating phase before epitaxial growth. This causes rounded V-groove tips, resulting in wider QWR's [16]. On the other hand, reproducible high-quality InGaAs–InAlAs QWR's were fabricated, making use of the "resharpening" of the Al-containing barriers [17]. However, Al-free structures promise a better long-term stability [18].

QWR's in V-grooves as the active region in lasers require an effective current confinement. This is achieved by pn-junctions [19] or by proton implantation [20].

In this paper, we present an InGaAsP–InP V-groove laser with an InGaAs single QWR active region grown by metal–organic vapor-phase epitaxy (MOVPE). We clearly demonstrate that a single QWR suffices for laser emission so that we do not have to have recourse to a multiple wire arrangement. For current blocking we use semi-insulating (s.i.) InP. Furthermore, the QWR is embedded in quaternary wave-guiding layers. We report on the laser concept and give evidence for its functioning by simulations. We describe the fabrication process of this structure and demonstrate laser action from a single InGaAs QWR. Finally, we discuss the origin of a second laser line that is observed in this structure.

Manuscript received September 15, 1999; revised January 7, 2000. This work was supported by the Volkswagen-Stiftung and by the Deutsche Forschungsgemeinschaft.

The authors are with the Institute for Semiconductor Technology, Technical University Carolo-Wilhelmina, D-38106 Braunschweig, Germany.

Publisher Item Identifier S 1077-260X(00)05091-7.

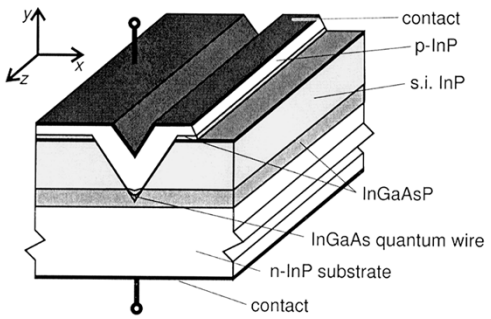

Fig. 1. Structure of QWR laser in InP substrate with V-shaped groove.

II. Device Structure and Optical Recombination

Fig. 1 shows the schematic cross section of the V-groove QWR laser in the material system InGaAsP–InP. Deposited on n^+-doped InP substrate, the first epitaxial layer stack consists of an n-doped InGaAsP layer and an s.i. InP layer. Subsequently, V-grooves are anisotropically etched with a standard photolithographic technique into these layers. With this technique, it is possible to transform micrometer sizes into the nanometer scale at the V-groove tip. Then, in a second epitaxial growth, the undoped InGaAs QWR is deposited into the tip of the V-groove. The active region (QWR) is covered by an undoped InGaAsP layer. This layer is followed by a p-doped InP layer and covered by a highly p-doped InGaAs contact layer. Metal contact stripes are patterned on the top of the structure and on the whole backside. The laser resonator is formed by $(01\bar{1})$ cleavage planes perpendicular to the QWR.

The quaternary layers around the QWR form an optical waveguide improving the optical confinement factor. S.i. material on both sides of the V-groove provides current blocking, which leads the carriers toward the QWR. Shunt connections are minimized in this way.

In order to verify this concept, we calculated the optical recombination rate by the finite-element method employing the program package ToSCA [21]. Fig. 2 shows the distribution of the optical recombination rate for the two-dimensional (2-D) geometrical structure shown in the x–y plane. For a better visualization, only the vicinity of the active region is shown as a detail of the whole laser structure. In order to obtain optical recombination, both electron and hole concentrations must be sufficiently high. Because of an efficient current carrier focusing on the active region enforced by the s.i. InP, the highest recombination rate is found at the QWR location in the tip of the V-groove, where electron and hole concentrations have their maxima. The simulation also shows a much reduced, though noticeable, optical recombination in the adjacent InGaAsP waveguiding layers. In comparison with the InGaAs QWR, the recombination rate is 40 times less because of the reduced electron and hole concentrations in this region.

The wave-guiding properties of the InGaAsP layers with a bandgap energy corresponding to 1.2-μm wavelength were calculated using the beam propagation method [22] with an exciting Gaussian beam. Fig. 3 shows the distribution of the amplitude of the electric field of the transverse electric (TE) fundamental mode as a gray-shaded plot of the cleavage plane. High

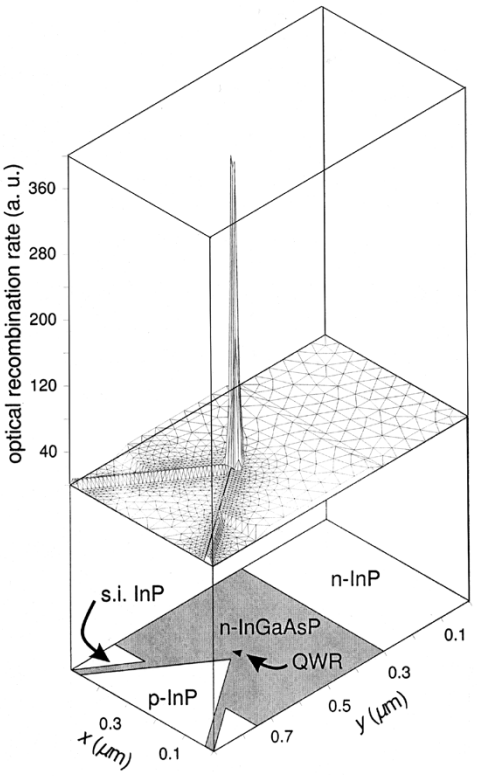

Fig. 2. Numerical simulation of the optical recombination rate within the core region around the quantum wire (cf. Fig. 1).

intensities are shown dark, low ones in bright. The QWR is superimposed as a black structure in the center. The filling factor of this structure with respect to the QWR is 0.1%.

III. Device Fabrication

We employ a two-step MOVPE process on an S-doped InP substrate $(N_D \approx 6 \times 10^{18}\ \text{cm}^{-3})$ with (100) $\pm$ 0.5° orientation and polished surface finish. The samples are chemically cleaned in boiling propanol, followed by a 5-min etching step in $H_2SO_4 : H_2O : H_2O_2$ (5 : 1 : 1) and a thorough rinsing in deionized water.

For MOVPE growth, we use a horizontal reactor with infrared (IR) heated susceptor. As sources, we employed trimethylindium and trimethylgallium as group-III precursors and arsine and posphine as group-V precursors, respectively. For doping sources, SiH_4, $(CH_3)_2Zn$, and $(C_5H_5)_2Fe$ are used for n- and p-type as well as s.i. layers, respectively. Hydrogen is the carrier gas. The total gas flow for all layers is approximately 8000 sccm. Growth temperature and total pressure are 640 °C and 20 hPa, respectively.

We start the growth with a 500-nm-thick InP buffer layer (Si-doped, $N_D = 5 \times 10^{17}\ \text{cm}^{-3}$). Subsequently, the lower InGaAsP wave-guiding layer (Si-doped, $N_D = 5 \times 10^{17}\ \text{cm}^{-3}$) and the s.i. InP current-blocking layer (Fe-doped, $N = 5 \times 10^{16}\ \text{cm}^{-3}$) are deposited.

The growth process is interrupted for etching of the V-grooves. A 40-nm electron-beam evaporated Ti film is used as an etching mask. Between 3- and 4-μm-wide stripes in

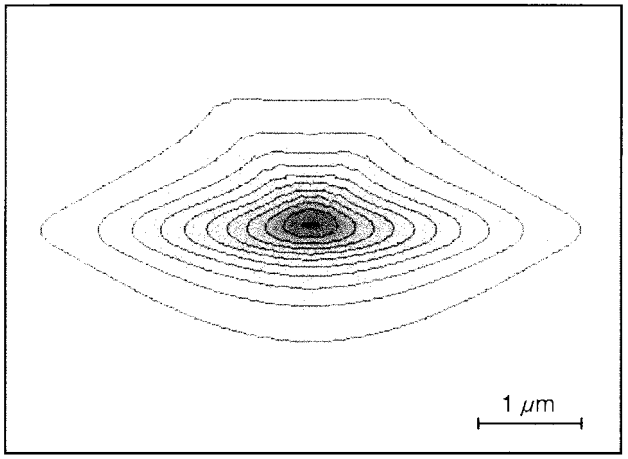

Fig. 3. Distribution of the amplitude of the electric field of the TE fundamental mode. The curves are isolines of the field intensity.

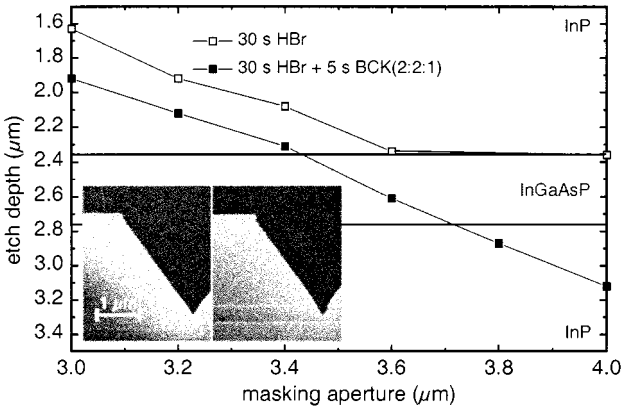

Fig. 4. Etch depth in an InP–InGaAsP layer stack in dependence of the Ti masking aperture.

$[01\bar{1}]$ direction are formed by the liftoff technique [23]. This step requires only conventional optical lithography as opposed to electron-beam lithography or ion implantation in other cases [10], [20]. Before the Ti evaporation, the samples were treated in an oxygen plasma for 20 s to remove photoresist residues [24].

A two-step wet-chemical etching process is used to fabricate high-quality V-grooves with $\{111\}$A sidewalls. During the first step, HBr (37%) is applied for 30 s, which is highly anisotropic for InP. In conjunction with the very low undercutting of the Ti-mask, this self-limiting process forms V-grooves in InP with $\{111\}$ sidewalls with a high pattern fidelity. The etching process is self-limited when the tip of the V-groove is formed. Its depth is only determined by the aperture of the Ti mask. This is shown by the open squares in Fig. 4. However, HBr does not attack InGaAsP so that the depth is stagnant if the width of Ti mask is large enough. The second etching step is performed for 5 s in $HBr : CH_3COOH : K_2Cr_2O_7$ (2 : 2 : 1) (BCK for short). Because the etching behavior of BCK for InGaAsP and InP is nearly the same, it is used to give the V-grooves their final shape. Beyond this, the $\{111\}$ sidewalls, showing ripples on their surfaces after the first etching step, are smoothed [25].

The tip positions of the V-grooves with different mask openings after this second etching step are marked by the solid squares in Fig. 4. For a width of 3.6 μm, the V-groove penetrates the whole s.i. InP top layer and ends just in the center of the underlying 400-nm-thick quaternary wave-guiding layer (dark gray). This optimum case is shown in the two inserts in the lower left corner where the cleaved V-grooves are depicted as scanning electron micrographs (SEM). In the right one, the InGaAsP is selectively etched by citric acid : H_2O_2 (7 : 1) [26] to visualize the material contrast. This leads to an edge on the $\{111\}$ plane at the interface, whereas in the left picture there is no discontinuity observable. Clearly visible in both pictures is the undercutting of the Ti mask during the second etching step. This is because of the isotropic etching behavior of BCK. Thus, this step is not self-limiting leading to the deviation of the solid squares from the open ones of the first step in Fig. 4. Nevertheless, this figure clearly demonstrates that it is possible to adjust the depth of the V-grooves in a controlled manner by the width of the Ti mask aperture.

Before the second epitaxial step, the patterned samples were etched in HF (5%, 10 s) and $H_2SO_4 : H_2O$ (5 : 1, 1 min). Compared with the first cleaning step, we omitted H_2O_2 to prevent the appearance of $\{311\}$ surfaces in the vicinity of the tip of the V-groove. To reduce the In mass transport, the first three layers, i.e., nominally 50-nm InP, 5-nm $In_{0.53}Ga_{0.47}As$, and 20-nm InP, were grown at 600 °C and 100 hPa. This forms a nearly lattice-matched InGaAs QWR in the tip of the V-groove [27]. Extending the growth of bare QWR's, we employ additional layers required for a laser structure. These layers were grown with standard parameters (640 °C, 20 hPa). During temperature increase, the growth of a 20-nm-thick InP layer is carried out to provide stable conditions. Covering the active region, the quaternary layer, the p-doped InP layer (cf. Fig. 1) and a p^+-doped InGaAs contact layer are grown.

After the growth, Ti–AuGe–Au is electron-beam deposited on the p^+-InGaAs top layer for the p-side ohmic contact. By means of standard photolithography, 100-μm-wide mesa-stripes are etched by using BCK. Finally, the sample is lapped from the backside down to about 100 μm. Ti–AuGe–Au is deposited to form the n-side ohmic contact. The samples are cleaved as laser bars of about 1-mm resonator length. The laser bars are fixed onto a Cu-holder by indium. The electrical contacts are bonded.

Fig. 5 shows an SEM picture of a mirror of such a device that was etched in citric acid : H_2O_2 (7 : 1) to obtain a material contrast. Because of the material-selective overetching, the QWR region is clearly visible. Its actual dimensions are 5.5×180 nm^2 [28].

IV. Results

At room temperature, we measured the near field of the devices by means of an IR microscope supplied with a PbS-vidikon camera. A filter with long wavelength transmittance above 1100 nm is used to suppress short wavelength radiation. In Fig. 6, the near field is shown for a cw current of 80 mA. The voltage across the device is about 1.1 V. The contour plot corresponds to the electroluminescence (EL) intensity of a single QWR. The highest intensity in the center

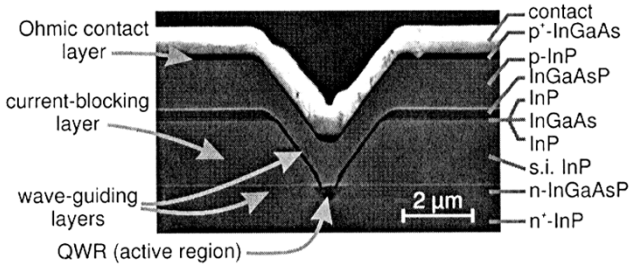

Fig. 5. Scanning-electron micrograph of a cleaved structure after material-selective etching.

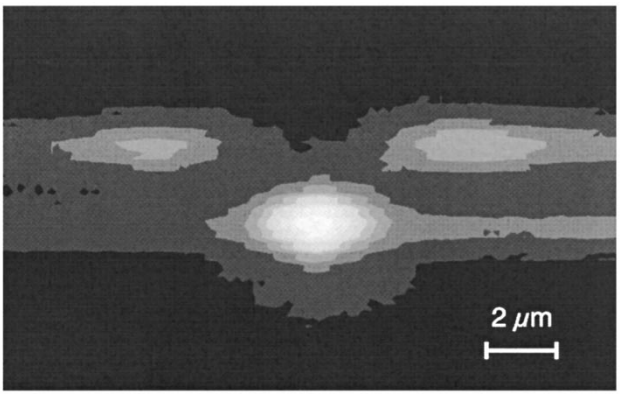

Fig. 6. Optical near field measured with an microscope supplied with an PbS-vidikon camera.

of the picture is located at the V-groove's tip. This is proven by superimposing the optical image with additional illumination of the cleavage plane. The measurement is in good agreement with the simulation of the optical recombination plot shown in Fig. 2. This experimental finding clearly demonstrates that the s.i. InP layer concentrates very efficiently the current into the QWR.

Additional maxima are visible, which are located in the quaternary layers grown on the (100) top surface at the edges of the V-groove. The embedding by InP (cf. Fig. 3) forms wave guides at the edges. This is probably the reason for observing EL intensity at these locations.

The same argument applies to the lower quaternary layer on both sides of the QWR. The distribution of the intensity shows a distinct anisotropy with respect to the x- and y-axis, respectively. This is in good agreement with the results of the simulation (see Fig. 3).

Beyond the near field, the EL spectra were examined at 15 K by means of a closed-cycle He-cryostat. We used a conventional setup with Peltier-cooled Ge detector and monochromator with a focal length of 640 mm with the lock-in technique. Electrical excitation by quasicontinuous pulses of 100-μs duration with a duty cycle of 30% are employed to reduce the thermal load.

Four spectra corresponding to four different currents ranging from 200 to 460 mA are displayed in Fig. 7. In the low current regime, three peaks are visible. As demonstrated by the PL-study on InGaAs–InP QWR's [27], the peak at 890 meV can be assigned to the QWR. The peak at 1066 meV originates from the quaternary material. This is corroborated by accompanying EL investigations with a sample consisting of a single QWL embedded into quaternary material as well as with the QWR-laser

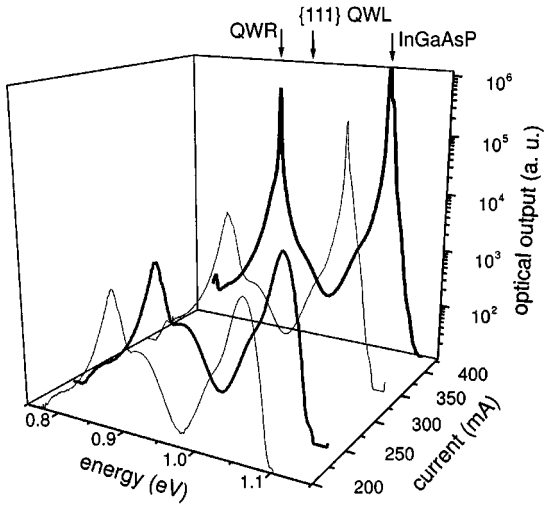

Fig. 7. Electroluminescence spectra of the structure of Fig. 5 for different driving currents as a parameter. The abscissa is the photon energy.

structure. In its low-energy shoulder, there is a peak shifted by 40 meV, which is probably from an electron acceptor transition in the upper quaternary layer. This may be related to an out-diffusion of Zn from the p-doped InP layer. Furthermore, a signal is visible at an energy of 928 meV. This signal originates from the thin quantum well, which is formed on the $\{111\}$ sidewalls [28]. With higher currents, the intensity of this peak increases only slightly, and no stimulated emission is recognized. On the other hand, the QWR- and InGaAsP-related peaks increase in intensity and simultaneously become narrower above 350 mA, which we attribute to laser action. These arguement clearly prove that the (100) QWL at the substrate surface is not optically active.

It follows from the spectra that there are two concurrent wavelength regions emitting stimulated radiation. The optical power-current curves as measured separately for each of the two main peaks elucidate this fact. We measured the optical power in a wavelength interval of 9 nm around the maxima as displaced in Fig. 8. For lower currents, the device behaves like an LED and the intensity increases because of spontaneous recombination. Laser action starts with the onset of stimulated emission at the threshold current. Two typical spectra for currents above threshold are represented in the upper part of Fig. 8. Their comb-like shape is typical for lasers with Fabry–Perot resonator. The individual peaks represent the longitudinal modes. Their wavelength separation is inversely proportional to the resonator length.

We explain the measurements by the model of two laser diodes (LD) in parallel, the quaternary LD and the QWR LD, respectively. The current shown in Fig. 8 is the total current through both diodes. Because of this reason, the threshold current of one LD cannot be determined directly, as is commonly done, from the sharp bend of the power-current characteristics. For the current-voltage characteristics, we assume for both diodes the validity of the ideal Shockley equation [29]

$$I = I_s\left(\exp\left(\frac{qV}{kT}\right) - 1\right) \tag{1}$$

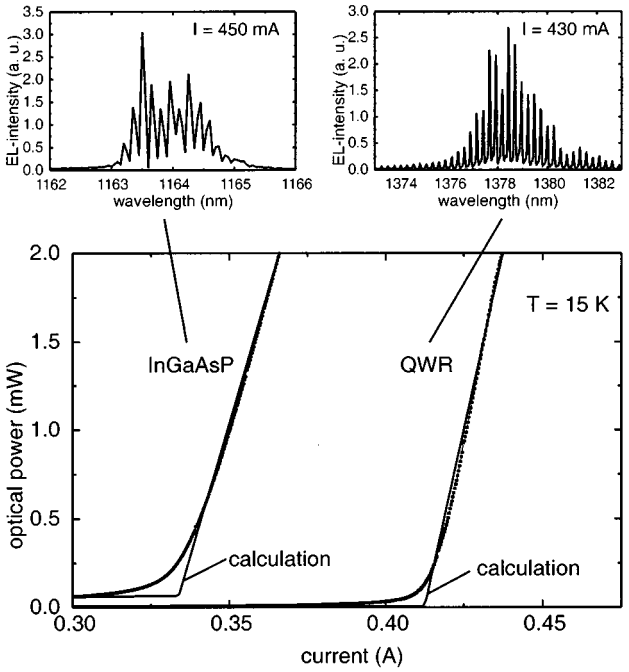

Fig. 8. Optical power versus driving current and the associated Fabry–Perot modes as measured wavelength resolved.

where

I_s reverse saturation current;

k Boltzmann's constant;

T temperature;

q electronic charge; and

V applied voltage being the same for both diodes.

With this in mind, the ratio of the reverse currents of both diodes is constant

$$\alpha = \frac{I_{s,\,\mathrm{quat}}}{I_{s,\mathrm{QWR}}}. \tag{2}$$

Below threshold, we presume the same quantum efficiency η_{LED} for both diodes. We assume a differential laser quantum efficiency η_d to calculate the optical output power. With fitting the model parameters, we obtain the thin curves in Fig. 8, which agree well with the experiment. We find that α is about 10; i.e., the current through the quaternary diode is a factor of 10 larger than that through the QWR. As a result, the threshold currents of 304 and 38 mA for the quaternary and QWR laser, respectively, show approximately the same ratio. However, the quaternary laser starts to emit at a lower total-current, because $\alpha = 10$. The differential quantum efficiencies resulting from our model are 6.2 and 98% for the quaternary and the QWR laser, respectively. This means that the fabricated QWR laser by itself shows promising properties that are concealed by the quaternary laser.

V. Conclusion

A new V-groove QWR laser concept is discussed that makes use of a s.i. current-blocking layer and additional wave-guiding layers in the alloy system InGaAsP–InP. We analyzed the concept by simulations. For the fabrication of the nanostructure, we take advantage of anisotropic etching. We developed a two-step wet-chemical etching process to form high quality V-grooves into a layer stack consisting of InP and InGaAsP. By employing anisotropic MOVPE growth on patterned substrates, we demonstrate the fabrication of a laser.

Laser action is shown from a single InGaAs QWR fabricated in an InP V-groove. A second laser line observed in the EL spectra is assigned to a parasitic quaternary laser. With a simple model, we separated both lasers and found very promising properties for the QWR laser.

Acknowledgment

The authors wish to thank T. Bulik for EL measurements, N. Riedel for technical assistance during the experiments, and D. Gvozdic for helpful assistance with the electrical simulations.

References

[1] M. Asada, Y. Miyamoto, and Y. Suematsu, "Gain and the threshold of three-dimensional quantum-box lasers," *IEEE J. Quantum Electron.*, vol. QE-22, pp. 1915–1921, 1986.

[2] Y. Arakawa and H. Sakaki, "Multidimensional quantum well laser and temperature dependence of its threshold current," *Appl. Phys. Lett.*, vol. 40, pp. 939–941, 1982.

[3] N. N. Ledentsov, "Quantum dot lasers: The birth and future trends," *Semiconductors*, vol. 33, pp. 946–950, 1999.

[4] W. Zhou, O. Qasaimeh, J. Phillips, S. Krishna, and P. Bhattacharya, "Bias-controlled wavelength switching in coupled-cavity $In_{0.4}Ga_{0.6}As$/GaAs self-organized quantum dot lasers," *Appl. Phys. Lett.*, vol. 74, pp. 783–785, 1999.

[5] G. Park, O. B. Shchekin, S. Csutak, D. L. Huffaker, and D. G. Deppe, "Room-temperature continuous-wave operation of a single-layered 1.3 μm quantum dot laser," *Appl. Phys. Lett.*, vol. 75, pp. 3267–3269, 1999.

[6] M. Higashiwaki, S. Shimomura, S. Hiyamizu, and S. Ikawa, "Self-organized GaAs quantum-wire lasers grown on (775) B-oriented GaAs substrates by molecular beam epitaxy," *Appl. Phys. Lett.*, vol. 74, pp. 780–782, 1999.

[7] S. T. Chou, D. E. Wohlert, K. Y. Cheng, and K. C. Hsieh, "The directionality of quantum confinement on strain-induced quantum-wire lasers," *J. Appl. Phys.*, vol. 83, pp. 3469–3472, 1998.

[8] S. Watanabe, S. Koshiba, M. Yoshita, H. Sakaki, M. Baba, and H. Akiyama, "Stimulated emission in ridge quantum wire laser structures measured with optical pumping and microscopic imaging methods," *Appl. Phys. Lett.*, vol. 73, pp. 511–513, 1998.

[9] S. Hara, J. Motohisa, and T. Fukui, "Self-organized InGaAs quantum wire lasers on GaAs multi-atomic steps," *Electron. Lett.*, vol. 34, pp. 894–895, 1998.

[10] T. Kojima, M. Tamura, H. Nakaya, S. Tanaka, S. Tamura, and S. Arai, "GaInAsP/InP compressively strained quantum-wire lasers fabricated by electron beam lithography and 2-step organometallic vapor phase epitaxy," *Jpn. J. Appl. Phys.*, vol. 37, pp. 4792–4800, 1998.

[11] M. Ishikawa, W. Pan, Y. Kaneko, H. Yaguchi, K. Onabe, R. Ito, and Y. Shiraki, "Polarization characteristics of crescent-shaped tensile-strained GaAsP/AlGaAs quantum wire-like lasers," *Jpn. J. Appl. Phys.*, vol. 37, pp. 1556–1558, 1998.

[12] T. Toda and Y. Nakano, "Room temperature operation of 1.5 μm InAsP/InP strained quantum wire DFB lasers fabricated by mass transport method," in *Proc. 11th Int. Conf. Indium Phosphide and Related Mater.*, Davos, Switzerland, May 16–20, 1999, pp. 17–20.

[13] S. Tiwari, G. D. Pettit, K. R. Milkove, F. Legoues, R. J. Davis, and J. M. Woodall, "High efficiency and low threshold current strained V-groove quantum-wire lasers," *Appl. Phys. Lett.*, vol. 64, pp. 3536–3538, 1994.

[14] S. Simhony, E. Kapon, E. Colas, D. M. Hwang, N. G. Stoffel, and P. Worland, "Vertically stacked multiple-quantum-wire semiconductor diode lasers," *Appl. Phys. Lett.*, vol. 59, pp. 2225–2227, 1991.

[15] T. G. Kim, X.-L. Wang, K. Komori, K. Hikosaka, and M. Ogura, "AlGaAs/GaAs quantum wire lasers fabricated by flow rate modulation epitaxy," *Electron. Lett.*, vol. 35, pp. 639–640, 1999.

[16] P. Bönsch, D. Wüllner, T. Schrimpf, H.-H. Wehmann, and A. Schlachetzki, "Growth of InGaAs/InP quantum wires on patterned substrates," in *Proc. 7th European Workshop Metal-Organic Vapor Phase Epitaxy Related Growth Tech. (EW-MOVPE VII)*, C1, Berlin, Germany, June 8–11, 1997.
[17] M. Kappelt, M. Grundmann, A. Krost, V. Türck, and D. Bimberg, "InGaAs quantum wires grown by low pressure metalorganic chemical vapor deposition on InP V-grooves," *Appl. Phys. Lett.*, vol. 68, pp. 3596–3598, 1996.
[18] J. Diaz, H. J. Yi, M. Razeghi, and G. T. Burnham, "Long-term reliability of Al-free InGaAsP/GaAs ($\lambda = 808$ nm) lasers at high-power high-temperature operation," *Appl. Phys. Lett.*, vol. 71, pp. 3042–3044, 1997.
[19] T. G. Kim, K. H. Park, S.-M. Hwang, Y. Kim, E. K. Kim, S.-K. Min, S.-J. Leem, J.-I. Jeon, J.-H. Park, and W. S. C. Chang, "Performance of GaAs–AlGaAs V-grooved inner stripe quantum well wire lasers with different current blocking configurations," *IEEE J. Quantum Electron.*, vol. 34, pp. 1461–1468, 1998.
[20] E. Kapon, S. Simhony, R. Bhat, and D. M. Hwang, "Single quantum wire semiconductor lasers," *Appl. Phys. Lett.*, vol. 55, pp. 2715–2717, 1989.
[21] "ToSCA two-dimensional semi-conductor analyze package," Weierstraß-Institut, Berlin, Germany.
[22] "BPM_CAD waveguide optics modeling software system," Optiwave Corp., Nepean, Ont., Canada.
[23] R. Klockenbrink, E. Peiner, H.-H. Wehmann, and A. Schlachetzki, "Wet chemical etching of alignment V-grooves in (100) InP through titanium or $In_{0.53}Ga_{0.47}As$ masks," *J. Electrochem. Soc.*, vol. 141, pp. 1594–1599, 1994.
[24] H.-H. Wehmann, T. Schrimpf, P. Bönsch, D. Wülner, D. Piester, A. Schlachetzki, and R. Lacmann, "Growth and characterization of InGaAs quantum-wires," in *Proc. 3rd Int. Wkshp. Heterostructure Epitaxy Devices (HEAD'97)*, P. Kordos and J. Novak, Eds. Dordrecht: Kluwer Academic, 1998, pp. 199–202. NATO Series 3/48.
[25] P. Bönsch, D. Wüllner, T. Schrimpf, A. Schlachetzki, and R. Lacmann, "Ultrasmooth V-grooves in InP by two-step wet chemical etching," *J. Electrochem. Soc.*, vol. 145, pp. 1273–1276, 1998.
[26] H.-H. Wehmann and A. Schlachetzki, "Technology and characterization of a photoconductive device on InP," in *Proc. ESSDERC'89*, A. Heuberger, H. Ryssel, and P. Lange, Eds. Berlin: Springer, 1989, pp. 491–494.
[27] T. Schrimpf, P. Bönsch, D. Wüllner, H.-H. Wehmann, A. Schlachetzki, F. Bertram, T. Riemann, and J. Christen, "InGaAs quantum wires and wells on V-grooved InP substrates," *J. Appl. Phys.*, vol. 86, pp. 5207–5214, 1999.
[28] T. Schrimpf, D. Piester, H.-H. Wehmann, P. Bönsch, D. Wüllner, A. Schlachetzki, C. Mendorf, and H. Lakner, "Preparation and characterization of InGaAs quantum wires on V-groove patterned InP," in *Proc. 11th Int. Conf. Indium Phosphide and Related Mater.*, Davos, Switzerland, May 16–20, 1999, pp. 507–510.
[29] S. M. Sze, *Physics of Semiconductor Devices*, 2nd ed. New York: Wiley, 1981.

Dirk Piester was born in Salzgitter, Germany, in 1969. He received the Diplom-Physiker degree from the Technical University Braunschweig, Braunschweig, Germany, in 1999. He is currently pursuing the Ph.D. degree from the University of Braunschweig.

He is currently with the Institute for Semiconductor Technology, Technical University, Braunschweig. His main work is focused on the characterization of quantum structures and optoelectronic devices.

Peter Bönsch was born in Göttingen, Germany, in 1968. He received the Diplom-Ingenieur degree from the Technical University Braunschweig, Braunschweig, Germany, in 1994. He is currently pursuing the Ph.D. degree from the Institute for Semiconductor Technology, Technical University Braunschweig.

His main field is the design and fabrication of semiconductor lasers, including the crystal growth by metal-organic vapor phase epitaxy.

Thomas Schrimpf was born in 1968 in Fulda, Germany. He received the Diplom-Ingenieur and Ph.D. degrees from the Technical University of Braunschweig, Braunschweig, Germany, in 1995 and 1999, respectively.

He is currently with the Institute for Semiconductor Technology, Technical University Braunschweig. His research interests are nanostructures on InP. He also works on the design and the characterization of semiconductor lasers.

Hergo-Heinrich Wehmann was born in Braunschweig, Germany, in 1956. He received the Diplom-Ingenieur and Ph.D. degrees from the Technical University Braunschweig, Braunschweig, Germany, in 1981 and 1987, respectively.

There he was involved in liquid phase epitaxy of InGaAsP on InP, from 1981 to 1984. In 1984, he joined the Heinrich-Hertz-Institut für Nachrichtentechnik, Berlin, Germany, where he worked on an integrated photoreceiver on InP. Since 1988, he has been with the Technical University of Braunschweig, where his main interest lies on the monolithic integration of InP-based optoelectronic devices with Si-electronics.

Andreas Schlachetzki was born in Breslau, Germany, in 1938. He received the Diplom-Physiker and Ph.D. degrees, both from the University of Cologne, Cologne, Germany, in 1964 and 1969, respectively. While at the University of Cologne, he worked in ferromagnetism and ultrasonics.

From 1970 to 1971, he investigated the magnetic properties of rare-earth-hydroxide single crystals at He temperatures at Becton Center, Yale University, New Haven, CT. In 1971, he joined the Research Institute of the German Post Office, Darmstadt, Germany, where he was involved in the epitaxial growth of GaAs, and in basic aspects of fast digital circuits utilizing the Gunn-effect in GaAs. In 1975, he worked for six months at the Electrical Communication Laboratory of Nippon Telegraph & Telephone, Tokyo. From 1976 to 1984, he was a Professor at the Technical University Braunschweig, where he worked on the growth of InGaAsP and its use for integrated optical receivers. From 1984 to 1987, he was a Professor at the Technical University Berlin and Head of the Division Integrated Optics at the Heinrich-Hertz-Institut für Nachrichtentechnik, Berlin. Since 1987, he has been the Head of the Institute for Semiconductor Technology, Technical University Braunschweig, where his main activities are in the field of monolithically integrated III-V components on Si substrates and Si micromachining.

Dr. Schlachetzki is a Member of the German Physical Society, the International Society for Optical Engineering (SPIE), and the Informationstechnische Gesellschaft.